

## A Summary of the Sardo, Ethiopia Earthquake of March 29, 1969.

Father Pierre Gouin summarized the study of the Sardo, Ethiopia, earthquake in his book, "Earthquake History of Ethiopia and the Horn of Africa", International Development Research Centre, Ottawa, Canada, 1979, 258 pp.

The following 14 pages were excerpted from the above mentioned book from page 128 to page 141.

### 1969/III-V (Serdo-Central Afar)

The town of Serdo (N 11°57', E 41°19') in the Danakil Desert was completely destroyed by an earthquake of magnitude  $m_b$  5.9. Out of a population of 420 people, 24 lost their lives and 167 were injured within minutes of the main shock at 2 p.m. (U.T. 11:05), 29 March; 15 others died later of injuries suffered during the collapse of their houses. Cracks, fissures, and subsidences appeared mainly in the plain southwest of the ridge on which Serdo was built. A second shock of magnitude  $m_b$  6.2 on 5 April at U.T. 02:18 (5 a.m.) opened three important faults about 8 km east of Serdo; one of these showed a vertical displacement of 75 cm downthrown to the northeast and a left lateral shear displacement of 65 cm. These faults crossed the highway. The same shock triggered rockslides along the highway and over quite a large area.

Over 250 aftershocks were recorded at the WWSS station in Addis Ababa; two reached magnitude  $m_b$  5.2.

Within 2 h of the disastrous shock of 29 March, help arrived from the nearby plantation in Tendaho and from the Christian Mission in Batie. The

dead were buried immediately after identification by their families; the survivors were injected against typhoid and cholera and evacuated to Logghia, 40 km west of Serdo, where a refugee camp was organized on the compound of the plantation's stores.

#### Sources

##### Descriptive

Gouin (1969, 7 and 17 April) (Official Reports on the situation in Serdo); Dakin et al. (1971); Searle and Gouin (1971a).

##### Instrumental

AAE Data File; BCIS; ISC; Fairhead and Girdler (1970); Gouin (1975); Sykes (1970); USCGS.

#### 1. Geographic Location of Serdo

The village of Serdo is situated near the geometrical centre of the "Afar triangle," midway between the port of Asseb on the Red Sea and Combolcia on the Ethiopian Plateau (Fig. 98). Its geographic coordinates are N 11.97°, E 41.31°; the elevation 400 m above sea level. Historically, Serdo grew up at the junction of the north-south caravan route from the salt plain in the Danakil Depression to the provincial capital Assayita, and the important east-west commercial trail from the Red Sea coast to the Ethiopian highlands.

In a way, Serdo was a unique town; its profile over the eastern horizon, outlined by a concrete water tower and other masonry buildings dominating the plain of Kurub from the top of an elevated ridge, was, to say the least, unexpected in the middle of the desert. Serdo owed its older masonry structures to the road construction company that built and maintained the Asseb-Combolcia highway in the late 1930s. Newer masonry buildings of dubious structural design have been added recently. The majority of the houses in the village were light wooden structures that were top-heavy and had 20-30 cm of earth and cinders for thermal insulation. Figure 99 identifies by name the different sectors (fedo, in the Afar language) prior to the 1969 earthquakes.

#### 2. Regional Tectonics and Geology

Central Afar is covered by volcanics (Fig. 100). Basalts form ridges, cinder cones, and extensive flows of both central and fissural origin, and rhyolite lavas and tuffs are associated with larger scattered centres and appear to overlie all but the youngest basalts. These volcanic flows are highly dissected by fresh normal faults into steeply sided blocks; the faults are variable in throw direction and the blocks generally tilt toward the SW or SSW. Between the fault-blocks lie planar areas formed by fluvial and lacustrine sedimentation.

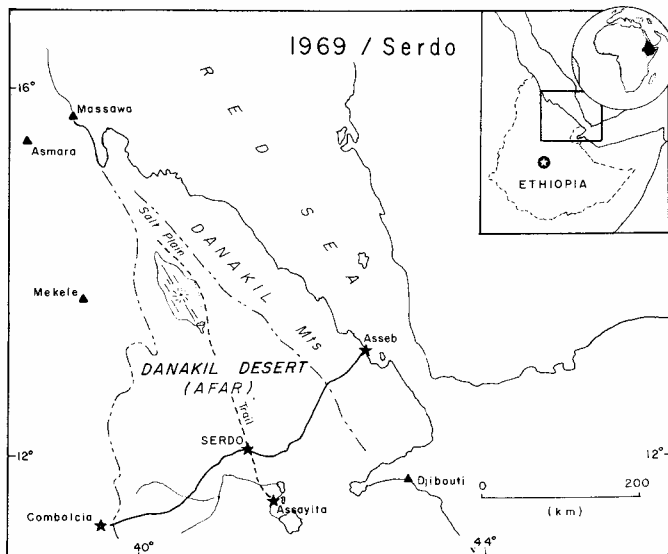


Fig. 98. Location map of Serdo in the Danakil Desert of northeastern Ethiopia.

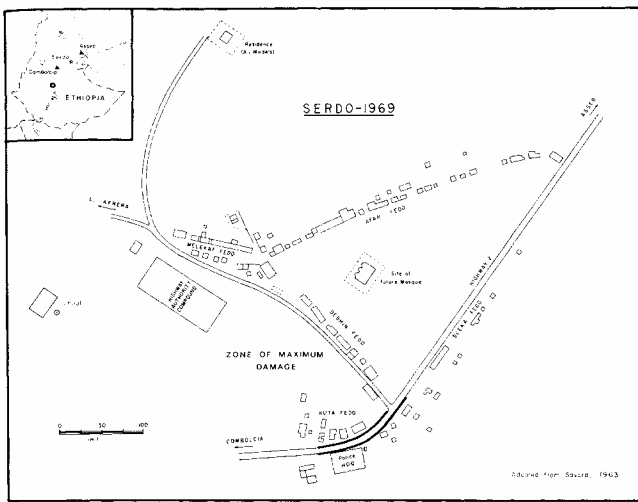


Fig. 99. The desert town of Serdo before the earthquakes. The basic layout was taken from the field notes of Georges C. Savard, head of the Department of Sociology, University of Addis Ababa.

Serdo was built on and around one of these fault-blocks trending N40W and tilted toward the southwest. The best masonry and concrete structures, such as the 30 ft (10 m) water tower, the police headquarters, and the highway authority compound, were erected on the ridge, a rhyolite block of almost vertical flow-banded structure (Fig. 101); the new school, a masonry structure too, was located in the plain northwest of the ridge (Fig. 103); the rest of the village was mainly concentrated in the plain to the east, enclosed between two ridges.

### 3. Regional Seismic and Volcanic Activity

#### Historical Survey

What is presently known of the seismic and volcanic activity in Aussa prior to 1969 is summarized in this paragraph. Details are to be found in the entries corresponding to the dates indicated; some of the epicentres are plotted in Fig. 100.

1608, 23 December (15 Remadam A.H. 1017): volcanic activity in the form of smoke coming out of the ground, east of Mt Waraba, near a lake, in Aussa.

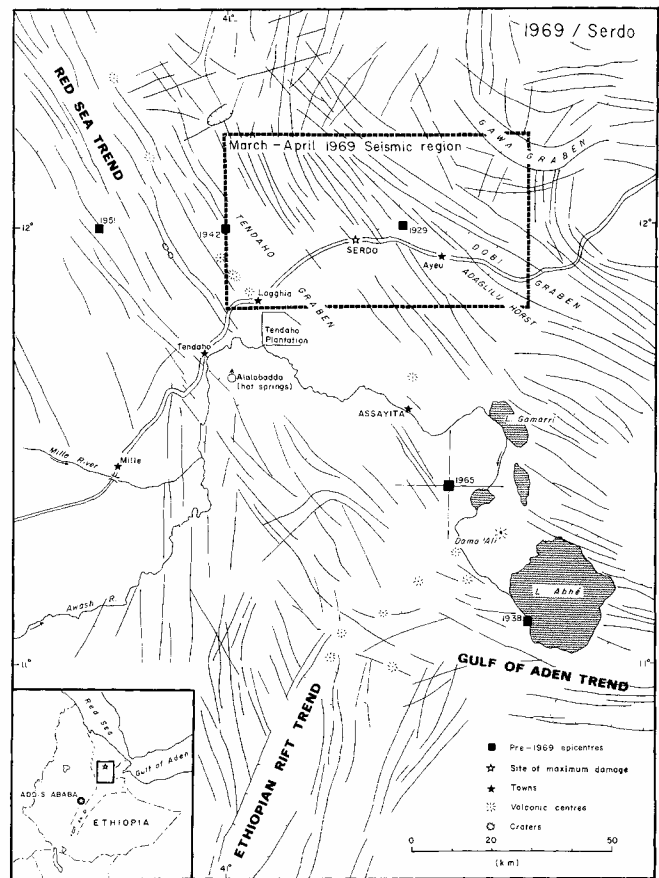


Fig. 100. Tectonic outline of Central Afar after Dakin et al. (1971). Plotted on this map are the epicentres known to have occurred before 1969. Standard error bars are indicated only for the epicentre of 1965; the others could not practically be determined.

1627 From 18 March to midsummer, seismovolcanic activity in Aussa destroyed all houses in Waraba; 50 people are presumed to have lost their lives.

1883 Strong earth tremors were felt near Mt Janghudi (N 10.5°, E 41.1°) and in Asseb (N 12.9°, E 42.7°). It is probable that the epicentral region was located in Central Afar.

1929, 18 May U.T. 01:02:15. Epicentre at N 12.0°, E 41.4°; M = 6.

1938, 27 September U.T. 02:31:51. Epicentre at N 11.1°, E 41.7°; M = 6.

1942, 18 November U.T. 12:01:20. Epicentre at N 12°, E 41°; M = 5½.

1951, 11 December U.T. 02:34:36. Epicentre at N 12°, E 40.7°.

1965, 7 June U.T. 13:43:57. Epicentre at N 11.43° ± 0.12°, E 41.48 ± 0.12°; h = 40 ± 29 km.

#### *Seismic Activity Near Serdo in 1969*

*Instrumental Data* — Of the 250 foreshocks and aftershocks of magnitudes  $\geq 3$  recorded during the period of seismic activity around Serdo, 12 have been listed by various agencies. Selected parameters are given in Table 4. Because the USCGS epicentre locations have been observed to best fit the AAE station recordings and were used in the determination of regional travel times (Searle and Gouin 1971), the residuals for P arrival times as calculated by USCGS are also indicated. The epicentral distances ( $\Delta$ ) given in Table 4 are reckoned from Addis Ababa.

The instrumental epicentres given in Table 4 are plotted in Fig. 104.

*Field Observations* — On 4 April 1969, a low-altitude air survey of the earthquake stricken area was made by USAID personnel. At the time, no apparently fresh geological surface disturbances were observed other than the cracks south of Serdo. On 5 April, the first of the three investigation teams headed by myself arrived at Serdo; the others followed in April–May 1969 and in 1970. During the field investigations, local residents and caravan teams were questioned, damage to structures examined, and all accessible tracks covered in the search for ground effects. Because the ruggedness of the terrain precluded access by ground vehicles to regions outside the main trails, the surveys are somewhat incomplete.

*Casualties.* The absolute number of casualties, some 40 dead and 160 wounded, is not excessively high, but if considered as a percentage of a total population of 420 people, it means that half of the population was either killed or wounded. Had the destructive shock of 29 March occurred before noon during school hours, the toll would have easily risen by another 20–30 children killed or injured. The total collapse of the school building leaves no doubt about it (see Fig. 101).

*Damage to Man-Made Structures.* All the masonry structures located on the Serdo ridge in the Kuta, Debhin, and Meleket *fedos*, including the highway authority compound and the police headquarters buildings,

were completely destroyed on 29 March (Fig. 103). The school located in the plain northwest of the town was likewise destroyed (Fig. 103). The reinforced-concrete water tower stayed up, but its brick facing fell off and the whole structure is now inclined by about 5° from the vertical in a SW direction. Houses with flexible wooden structures, unless heavily topped with earth, suffered much less. Only two structures stayed virtually intact; they were entirely wooden: the house of H.E. Bitweded Ali Mirah, and the Telecommunications Office (Fig. 102).

In the region of Serdo, as well as 8 km to the east in the vicinity of faults F<sub>1</sub> and F<sub>2</sub> described below, bridges and culverts were damaged (main structures cracked, head walls broken, supporting walls fissured, etc.).

The damage was concentrated in a rather restricted area. No damage was reported from Logghia, 40 km southwest of Serdo, one small crack was observed at Ayeu, 25 km to the northeast; on the Tendaho Cotton Plantation, at about the same distance from Serdo as Logghia, a few adobe houses collapsed (Fig. 103), some walls were fissured, and cracks ran across the pavement of the club house, the fish pool, and the swimming pool. They are discussed below under “cracks.” The damage at the plantation occurred on 5 April.

#### *Geologic Surface Effects*

*Cracks.* In this context, “cracks” are defined as small tensional fissures with no significant vertical or lateral displacement. Several were observed in the tarmac of the highway. They were up to 20 metres long, 30 cm wide and about 20 cm deep. All but two were parallel to the road. In Serdo, one was perpendicular to the road but parallel to a nearby culvert; it was certainly caused by the dislocation of the concrete culvert structure from the road pavement. The other was located about 0.5 km west of Serdo; its strike (N60W) made an angle of about 10° with the axis of the road. All these cracks, with the possible exception of the last one, are believed to have been entirely controlled by slumping of the highway understructure; they are not considered to have any directional tectonic significance.

A crack, 5–10 cm wide, striking north-south, opened at the northwest end of the Serdo ridge, running through the ground and the masonry foundation of the main building on the highway authority compound. This crack was due to slumping of the foundation structure.

Cracks not on the surface of the road, and therefore of probable significance as regards directional tectonic trends, were observed at two locations: (1) about 500 m south of the town; and (2) about 8 km to the east of it. At both sites, they occurred in loose sediments. At location (1) in the sediment covered plain south of Serdo, cracks (C<sub>1</sub>) developed in a zone about 400-m long by 10-m wide (Fig. 105B). Individual cracks were 0.5–3.0 m long, 15–20 cm deep, and 1–20 cm wide. The centre of the zone subsided by 20–25 cm. The general trend of the zone was N40W; it changed to roughly east-west at its northwestern end. The direction of individual cracks

Table 4. Parameters for the 12 largest events during the Serdo sequence.

		$H_0$	Coordinates		$h(\text{km})$	St.	$m_b$	$M_s$	$\Delta(\text{km})$	O-C	
(1)	29 Mar	CGS	$09:15:54.1 \pm 0.17$	$11.97 \pm 0.03^\circ$	$41.18 \pm 0.03^\circ$	33	72	5.8	6.3	420	-1.6
		ISC	$09:15:54 \pm 1.0$	$11.91 \pm 0.03^\circ$	$41.21 \pm 0.03^\circ$	$35 \pm 10$	204	5.9		417	
		JED		$12.02^\circ$	$41.18^\circ$					426	
		PG		$11.93^\circ$	$41.27^\circ$					423	
(2)	29 Mar	CGS	$11:04:47.9 \pm 3.7$	$11.96 \pm 0.04^\circ$	$41.29 \pm 0.055^\circ$	$4 \pm 22$	54	5.6		427	-0.5
		ISC	$11:04:52 \pm 1.1$	$11.92 \pm 0.03^\circ$	$41.36 \pm 0.032^\circ$	$35 \pm 11$	166	5.5		429	
		JED		$12.03^\circ$	$41.24^\circ$					429	
		PG		$11.94^\circ$	$41.30^\circ$					426	
(3)	29 Mar	CGS	$11:07:30.0 \pm 0.3$	$11.99 \pm 0.03^\circ$	$41.21 \pm 0.85^\circ$	33	21	5.3	5.8	424	
		ISC	$11:07:45 \pm 6.0$	$12.01 \pm 0.07^\circ$	$41.1 \pm 0.14^\circ$	$164 \pm 56$	55	4.9		418	
		JED		$12.06^\circ$	$41.48^\circ$					449	
		PG		$11.91^\circ$	$41.57^\circ$					443	
(4)	29 Mar	CGS	$13:08:11.4 \pm 3.9$	$11.94 \pm 0.03^\circ$	$41.52 \pm 0.09^\circ$	$4 \pm 23$	23	5.1		495	-0.7
		ISC	$13:08:17 \pm 1.2$	$11.94 \pm 0.04^\circ$	$41.31 \pm 0.05^\circ$	$43 \pm 12$	88	5.1		427	
		JED		$12.03^\circ$	$41.41^\circ$					441	
		PG		$11.85^\circ$	$41.49^\circ$					433	
(5)	29 Mar	CGS	$18:30:42.2 \pm 0.4$	$12.00 \pm 0.08^\circ$	$41.38 \pm 0.12^\circ$	33	8	4.6		437	
		ISC	$18:30:49 \pm 5$	$11.87 \pm 0.09^\circ$	$41.40 \pm 0.13^\circ$	$95 \pm 52$	19			427	
		JED		$12.01^\circ$	$41.34^\circ$					435	
		PG		$11.89^\circ$	$41.43^\circ$					431	
(6)	05 Apr	CGS	$02:18:29.9 \pm 1.9$	$12.15 \pm 0.03^\circ$	$41.20 \pm 0.04^\circ$	$17 \pm 14$	46	6.2	6.1	437	-2.3
		ISC	$02:18:30 \pm 2.8$	$12.00 \pm 0.04^\circ$	$41.35 \pm 0.04^\circ$	$19 \pm 20$	175	5.8		435	
		JED		$12.19^\circ$	$41.13^\circ$					448	
		PG		$12.12^\circ$	$41.26^\circ$					446	
(7)	05 Apr	CGS	$20:06:23.8 \pm 0.4$	$11.91 \pm 0.08^\circ$	$41.14 \pm 0.11^\circ$	33	6	4.3		412	+0.3
		ISC	$20:06:24 \pm 2.8$	$12.0 \pm 0.15^\circ$	$41.2 \pm 0.20^\circ$	$32 \pm 33$	13			424	
		JED		$12.02^\circ$	$41.10^\circ$					420	
		PG		$11.95^\circ$	$41.19^\circ$					419	
(8)	05 Apr	CGS	$20:14:35.9 \pm 0.4$	$12.03 \pm 0.04^\circ$	$41.47 \pm 0.07^\circ$	33	19	4.9	5.2	447	+1.2
		ISC	$20:14:41 \pm 1.3$	$12.02 \pm 0.05^\circ$	$41.28 \pm 0.07^\circ$	$70 \pm 14$	35	4.8		431	
		JED		$12.11^\circ$	$41.49^\circ$					454	
		PG		$11.96^\circ$	$41.59^\circ$					449	
(9)	06 Apr	CGS	$16:51:45.5 \pm 2.0$	$12.03 \pm 0.04^\circ$	$41.12 \pm 0.06^\circ$	$20 \pm 15$	39	5.2	5.4	421	-0.1
		ISC	$16:51:47 \pm 1.1$	$11.99 \pm 0.03^\circ$	$41.40 \pm 0.039^\circ$	$41 \pm 11$	104	5.1		437	
		JED		$12.07^\circ$	$41.11^\circ$					424	
		PG		$12.00^\circ$	$41.21^\circ$					425	
(10)	07 Apr	CGS	$06:23:53.4 \pm 1.2$	$11.98 \pm 0.10^\circ$	$41.28 \pm 0.08^\circ$	33	14	4.6		428	-0.3
		ISC	$06:23:55 \pm 1.8$	$11.92 \pm 0.10^\circ$	$41.40 \pm 0.09^\circ$	$58 \pm 20$	24			432	
		JED		$12.04^\circ$	$41.30^\circ$					434	
		PG		$11.93^\circ$	$41.39^\circ$					432	
(11)	08 Apr	CGS	$02:13:58.7 \pm 1.3$	$11.93 \pm 0.06^\circ$	$41.37 \pm 0.07^\circ$	$34 \pm 13$	18	4.8		430	-0.4
		ISC	$02:14:01 \pm 1.1$	$11.88 \pm 0.05^\circ$	$41.42 \pm 0.05^\circ$	$56 \pm 12$	52	4.8		430	
		JED		$12.02^\circ$	$41.37^\circ$					438	
		PG		$11.90^\circ$	$41.62^\circ$					446	
(12)	05 May	CGS	$02:45:38.9 \pm 1.3$	$11.94 \pm 0.08^\circ$	$41.26 \pm 0.06^\circ$	$35 \pm 15$	20	5.2	5.0	423	
		ISC	$02:45:40 \pm 1.5$	$12.07 \pm 0.04^\circ$	$41.34 \pm 0.06^\circ$	$38 \pm 15$	83	4.9		440	
		JED		$12.01^\circ$	$41.28^\circ$					431	
		PG		$11.90^\circ$	$41.37^\circ$					428	

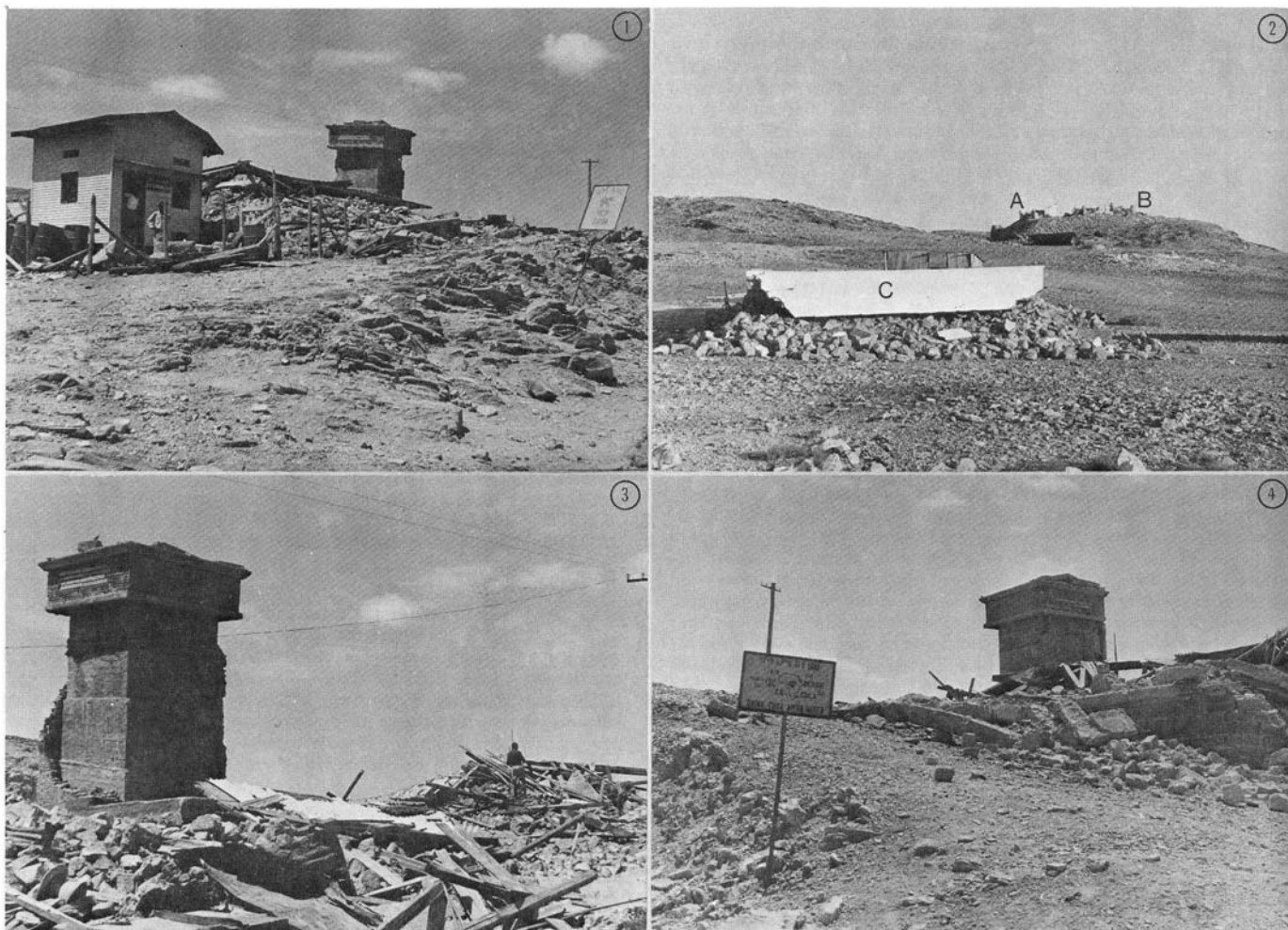


*Fig. 101. Ruins of Serdo after the main shock of 29 March 1969. Nothing was left intact except the wooden shack of the telecommunications board (upper left, plate 1) and a wooden house north of the town. In Afar Fedo, the light structures stood the shocks. On the upper right of plate 2, the silhouette of the section of the village erected on the Serdo ridge can be seen. The letter A locates the highway authority compound, B the reinforced concrete water tower leaning about 5° SW, and C the village school that had housed 30–35 students 2 h earlier. Plates 3 and 4 show the water tower, deprived of its brick facing, but still standing among the ruins of the post office and police headquarters.*

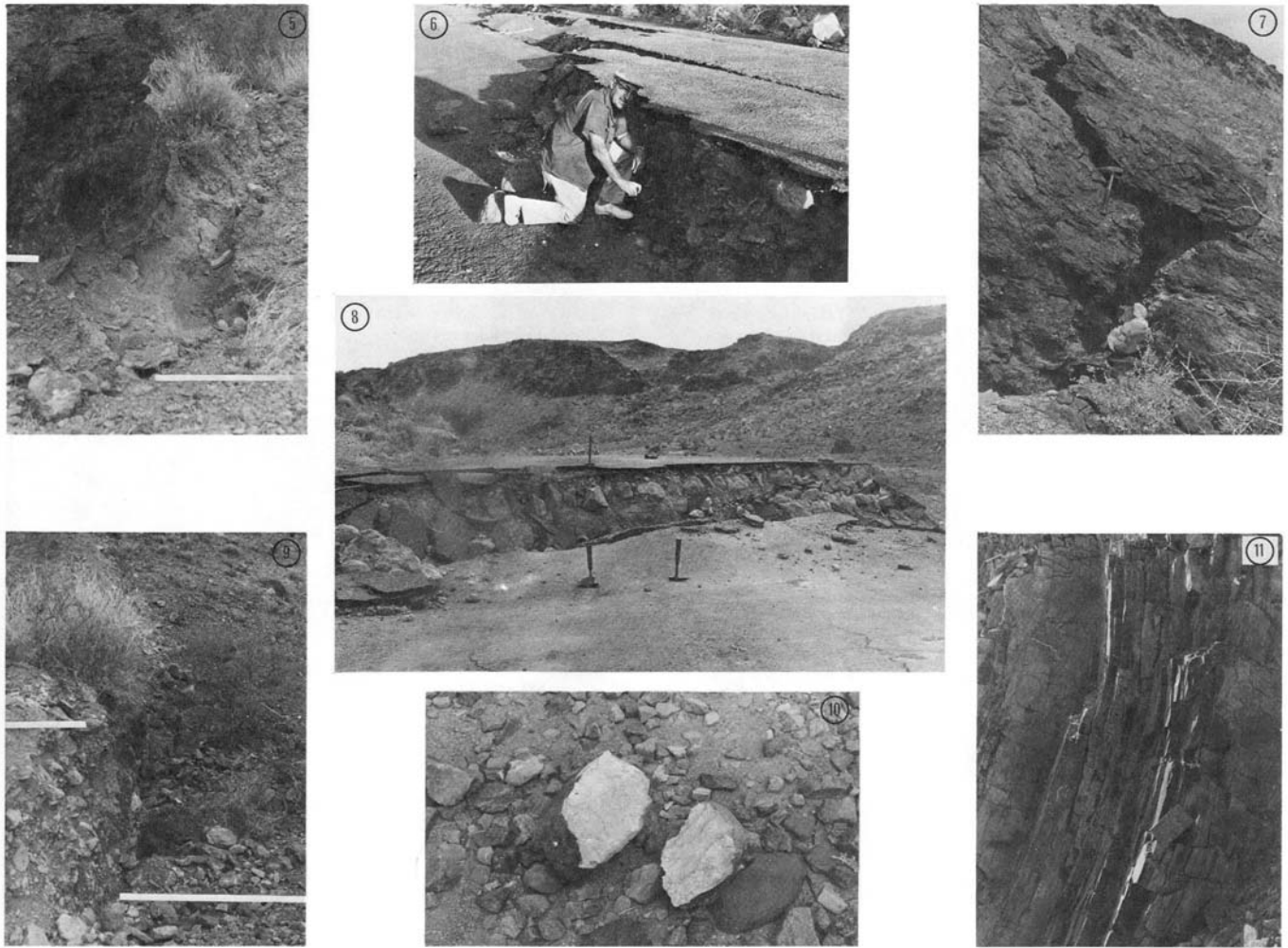


Fig. 102. Fault  $F_1$ , some 8 km east of Serdo. It developed on 5 May (striking N40W subparallel to the ridge axis) and had a vertical displacement measured on the highway of about 75 cm and a left-lateral displacement of about 65 cm. Northwest of the highway  $F_1$  could be traced for about 1 km before it became indistinct among the hillwash (plates 5 and 9). Plate 6. Fault  $F_2$  crossing the road obliquely. Fracturing plus slumping reached a vertical displacement of some 95 cm. Plate 7. A broken boulder along the fault. Plate 10. A rock apparently freshly broken by impact on a harder specimen after having been projected up by a vertical seismic motion. The point of impact was clearly observed (also see plate 19). Plate 11. A close-up of the north wall of the road-cut through Serdo ridge showing the almost vertical and highly contorted flow-banded rhyolite that forms the ridge.

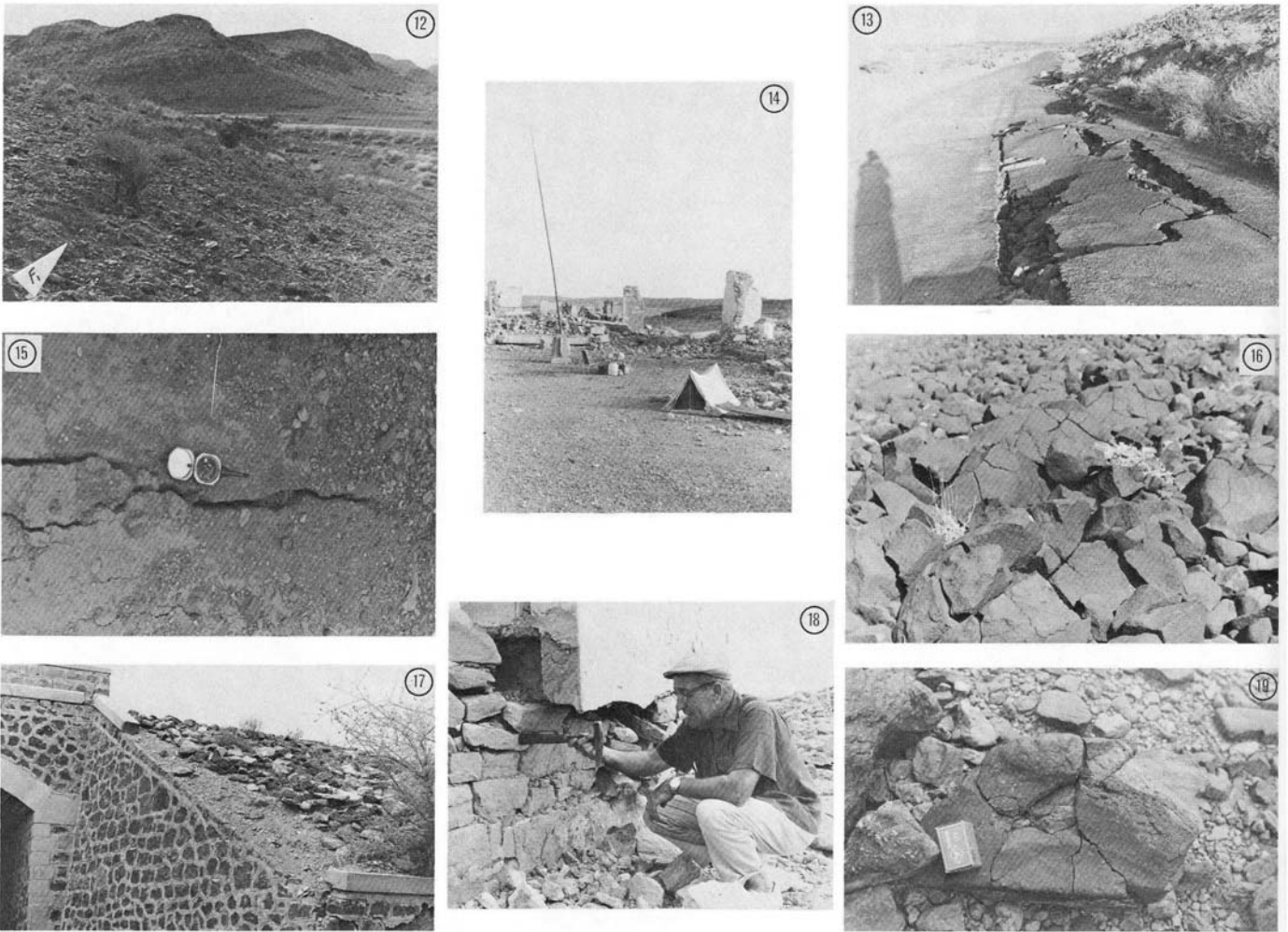


Fig. 103. Plate 12. Fault  $F_1$  along the hillside; direction  $N40W$ . Plate 13. Vertical differential displacement along the highway. Plate 14. Ruins of the highway authority compound. Notice the steel flagpole, 7.5 cm at its base, inclined to the SW. The cement base was cracked, and the local people ascertained that the bending of the flagpole was a result of the earthquake. Plate 15. Cracks in the tarmac; they tend  $N30W$ . Plate 16. Whole field of freshly broken boulders about 20 km north of Serdo. Another site where broken boulders, were found was about 10 km north of Serdo, on the prolongation of  $F_1$ . Plate 17. Upheaved riprap highway slope near  $F_3$ . The bridge sill and headwall had cracked, the capped section of the retaining wall had fallen, and the wall itself had fissured. Plate 18. An example of apparent rotational motion. Plate 19. Freshly broken rock showing the point of impact of a second boulder projected by sudden vertical seismic motion.



in this  $C_1$  zone varied within  $\pm 30^\circ$  of the general trend. Local people reported that these cracks had developed on 29 March. They occurred in loosely packed alluvium overlying gravel beds, thus they were probably entirely due to compaction caused by the tremors and merely reflected the surface and underground regional topography.

At location (2) about 8 km east of Serdo and close to the main road (Fig. 105C) a zone of cracks ( $C_2$ ) occurred in loose hillwash at the foot of a steep escarpment. These cracks appeared to be associated with fresh normal faulting that resulted from the shock of U.T. 02:18:29.9 on 5 April. This faulting is described below under "faults." The cracks were similar in length, width, and depth to those found at location (1). They did not, however, lie in a continuous band but occurred as individual, isolated units or in short discontinuous bands. Their general trend was N40W, but variations of  $\pm 60^\circ$  were observed.

A crack was observed running through the hard soil floor and the baking oven of the Tehame Tekle Hotel in Ayey, 25 km east of Serdo. Its direction was N60–70W.

Other cracks were observed at the Tendaho Cotton Plantation: one ran through the east porch of the club house in a N80E direction (this crack was reported to be existing before 5 April and to have merely widened on 5 April); a second one cut through the structure of the fish pool in a N40W direction; a third ran along the joints of the walls in the swimming pool. All occurred on 5 April.

*Faults.* "Faults" in this context are fractures that show appreciable vertical and/or lateral displacement. Fresh faulting was observed at three positions about 8 km east of Serdo along the main road. Positions  $F_1$  and  $F_2$  are indicated on Fig. 104 and 105. The fault  $F_3$ , about 1 km east of  $F_2$ , is beyond the area of the maps.

Fault  $F_1$ , striking N40W, was almost perpendicular to the road and parallel to a major N40W fault scarp (Fig. 105C). Its vertical displacement, measured at the road, was about 75 cm and it showed a left lateral displacement of about 65 cm (50 cm was given in the preliminary report to Smithsonian Center for Short-Lived Phenomena, card 493/1969). This fresh fault was traced for about 100 m to the southeast of the road where it deteriorated into the series of cracks described above for location (2). To the northwest of the road, the fault continued for at least 1 km, becoming less distinct with increasing distance from the road, until it was eventually obscured by hillwash. The second fault ( $F_2$ ), striking N50W, cut obliquely across the main road about 200 m east of  $F_1$ .  $F_2$  had a vertical displacement of 90–95 cm, showed no detectable lateral displacement, and could not be traced on either side of the road (Fig. 105). About 500 m east of  $F_2$  one small fault ( $F_3$ ) showing a left lateral displacement of 10 cm was observed in the tarmac of the road. The strike of this fault was N50W, almost perpendicular to the road.

All the faults described above developed in the morning of 5 April.

*Rockslides.* One rockslide occurred 4 km east of Serdo; two more, on the southeast side of the Dobi graben (see Fig. 105) at 39 and 40 km east of Serdo by road. They were triggered during the afternoon of 5 April. Other rockslides and landslides occurred at different places as signaled by clouds of dust rising above the hills; their location could not be identified because the sites were inaccessible by land vehicles.

*Ground motions (horizontal, rotational, and vertical)*

(1) *Horizontal motion:* It was reported by the villagers of Serdo that on 29 March, people, animals, and walls were projected in an eastward or northeastward direction. The permanent inclination toward the southwest of both the 3-inch (7.5-cm) steel flagpole of the highway authority compound and the reinforced concrete tower (Fig. 101; Fig. 102) shows that their bases were suddenly jerked northeastward.

(2) *Rotational motion* was observed on the highway authority compound: one end of a 2-m long wall was rotated  $10^\circ$  counterclockwise. Such an angle of rotation may partly be due to unequal dislocation of the masonry.

(3) *Vertical displacements:* Fig. 103 shows two small freshly broken rocks, photographed in situ, near the main fault  $F_1$ . The fractures in the rocks were apparently caused by sudden upwards motion. Number 16 shows a rock sample that must have been projected upward and broke when it fell on a harder rock; number 19 shows the point of impact where a projected rock hit a small bolder and cracked it.

On either side of fault  $F_1$ , which was located 8 km east of Serdo, were first-order vertical control benchmarks: M35 at km 5.41 and L35 at km 9.92. In 1960, the USCGS survey team measured a difference in elevation of 450.3 cm between the two sites (USCGS 1957–1961, Ethiopian Geodetic Survey, Washington); in 1970, our releveling showed a difference of 510 cm, representing an increment of 60 cm over a 10-year period. This increment is presumed to have occurred rather suddenly at the beginning of May 1969. The regional extent of the subsidence with respect to the mean sea level reference in Asseb is unfortunately not known; there was no possibility of remeasuring a few hundred kilometres of first-order elevation profile.

*Other phenomena observed during the 1969 period of seismic activity.*

*Noises.* On 29 March, noises like explosions were reported in both Serdo and Dubti, near the Tendaho Plantation; people were under the impression that they were coming from the Alalobadda geothermal region (Fig. 100). Investigation of the Alalobadda site revealed no sign of explosion such as freshly broken rocks or a change in the level of the springs.

*Smoke.* "Smoke" was reported as having been observed over the hills surrounding Serdo, both on 29 March and 5 April. At the same time there

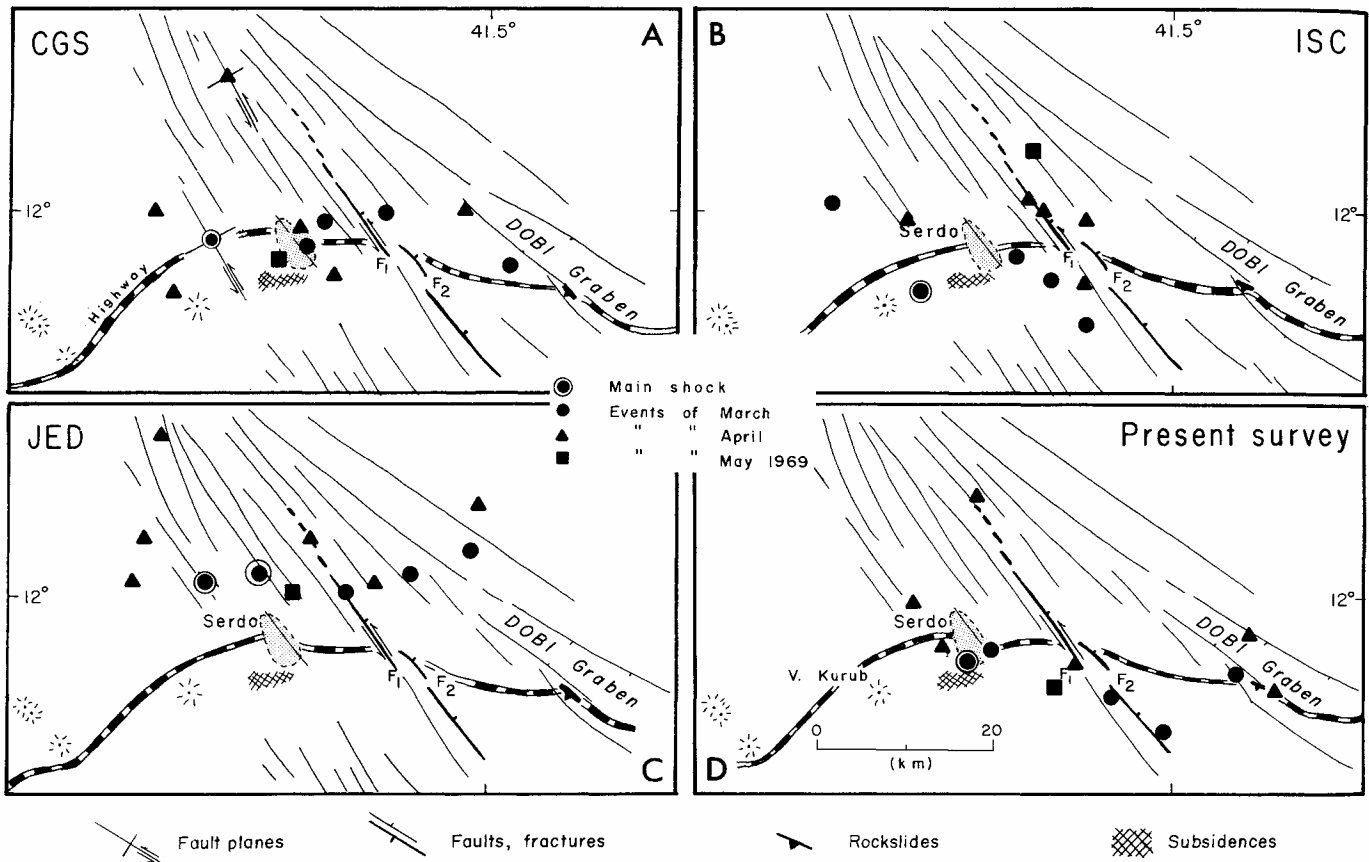


Fig. 104. Distribution plots of the Serdo epicenters as determined by: (A) the USCGS; (B) the International Seismological Center; (C) Fairhead and Girdler; and (D) Gouin.

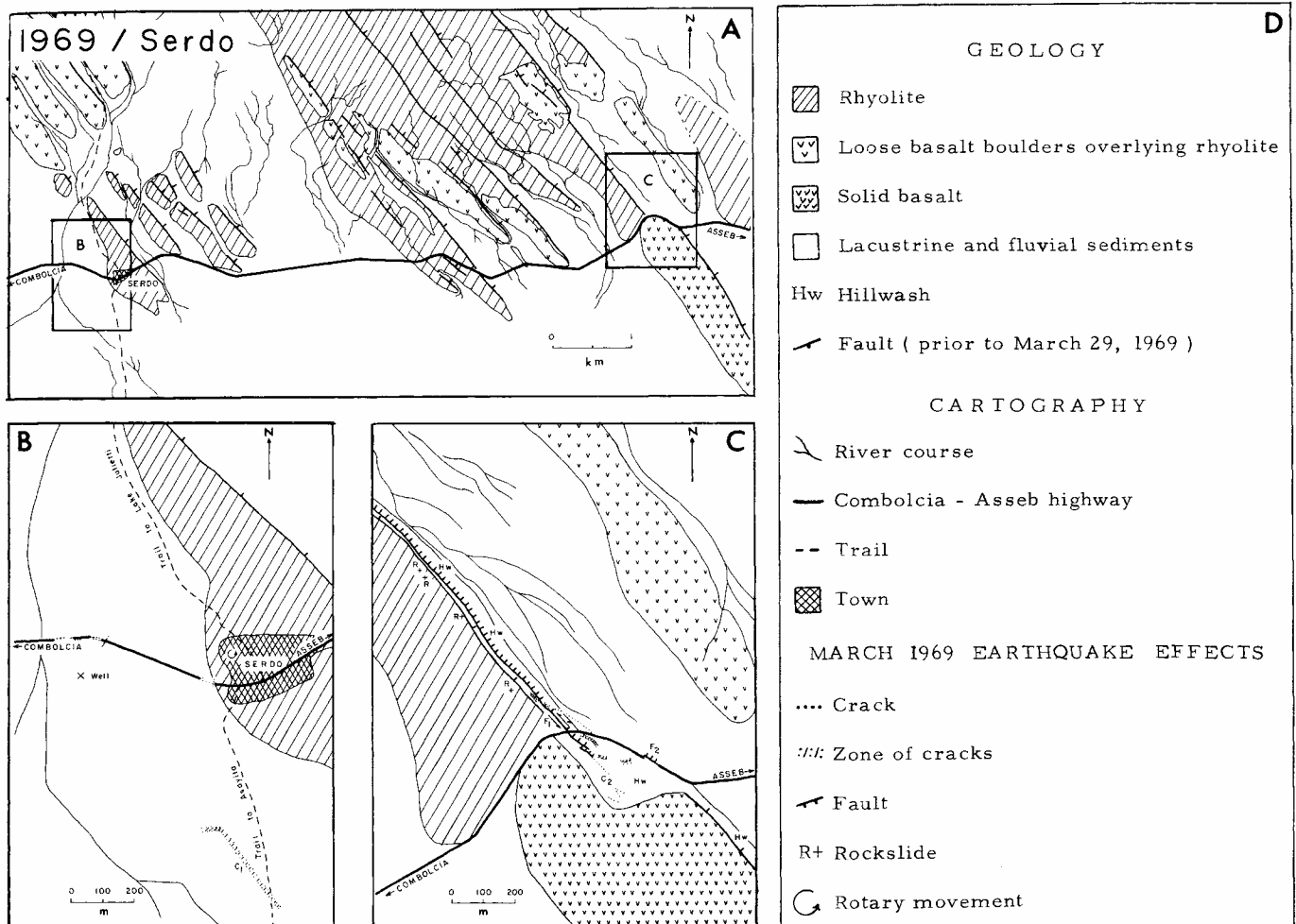


Fig. 105(A). Geological map of Serdo and vicinity. (B and C). Location of the surface effects observed during the March-May earthquake sequence of 1969 (after Dakin et al. 1971).

were rumors of renewed volcanic activity; the rumors were unfounded and it is believed that the "smoke" was dust thrown up by rockslides.

*Smell.* On 29 March, sulfurous smells were reported from Serdo. No satisfactory explanation was found.

*Seismic Activity Around Serdo After 1969*

The quiescent level of seismic activity in Central Afar did not in any way appear altered by the 1969 sudden outburst. Shocks at epicentral distances between 420 and 450 km from a northeasterly direction — the distance of Serdo from Addis Ababa is 432 km at an azimuth of 041° — were, and still are, observed at about the same rate as before on AAE seismograms. Their epicentral locations can be more accurately determined since the installation of the seismic network in Djibouti.

A microseismic survey of the Serdo-Tendaho region was conducted by the University of Durham during the period of February–September 1974. A network of four stations recording on magnetic tape was installed at Mille (N 11.420°, E 40.752°), Det Bahri (N 11.561°, E 41.208°), Tendaho (N 11.690°, E 40.958°), and Serdo (N 11.957°, E 41.359°). The location and geometry of the network are given in Fig. 106.

Due to technical and climatological problems, the operation of the network was intermittent; the records are good for 124 days. During that

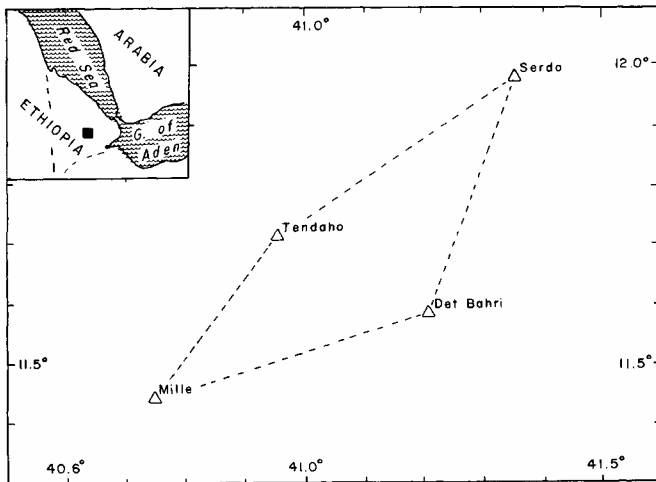


Fig. 106. Geographical location of the Durham seismic network in Central Afar during the microearthquake survey of 1974.

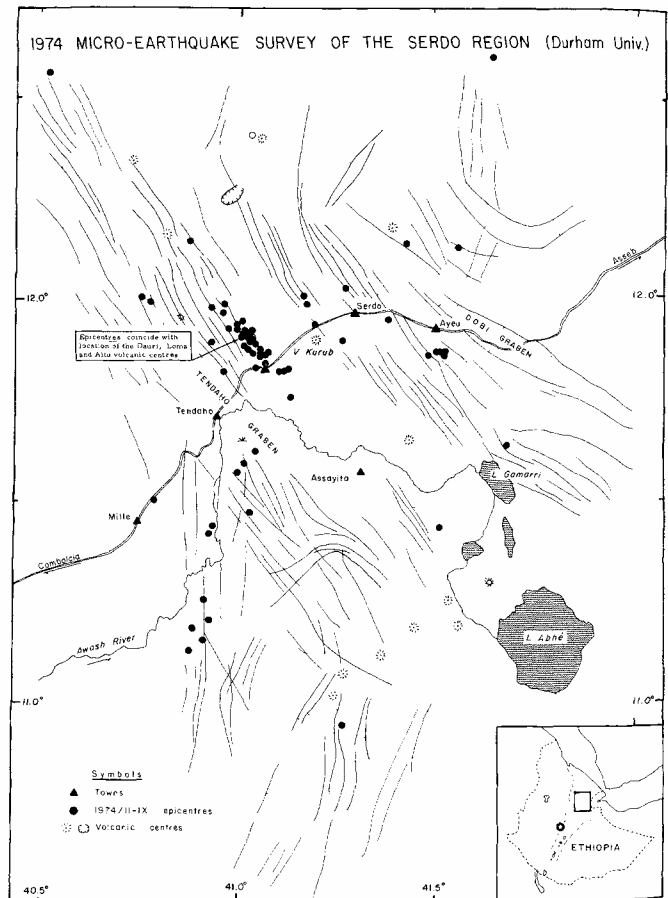


Fig. 107. Low magnitude epicentres in the Serdo region located from February to September 1974 by the Tendaho local network. No calculated focal depth exceeded 10 km. This 1974 epicentre plot is introduced here as a complement to the 1969 Serdo seismicity map.

period, over 400 local shocks were recorded. Epicentres could be determined for about 200 events and accurate depths for 25. More accurate details are intentionally not given here because the survey was part of a PhD research project by William G. Rigden and his thesis has not been defended yet.

Figure 107 is the location plot of the low magnitude epicentres determined by the Tendaho local network in the Serdo region.

#### 4. Notes on Some Earthquake Source Parameters During the 1969 Serdo Sequence

**Focal Depths** — Although focal depths computed from teleseismic records are always subject to rather high uncertainties mainly resulting from “unknowns” neglected in the seismic earth models used, nevertheless, the values published by reliable agencies give a clue about the depth range of hypocentres in determined seismic regions. In the case of the 1969 Serdo earthquakes, the published values ranged between  $4 \pm 22$  km and Normal for the USCGS,  $32 \pm 33$  and  $164 \pm 56$  km for ISC (Table 4). When one looks at the local crustal structure deduced from deep seismic soundings (Berckhemer et al. 1975, profile IV, p. 99 — see following table and Fig. 108) hypocentres deeper than 50 km become suspicious. The Durham University survey revealed that out of 25 focal depths that could be determined in the Serdo area from February to September 1974, none was larger than 10 km.

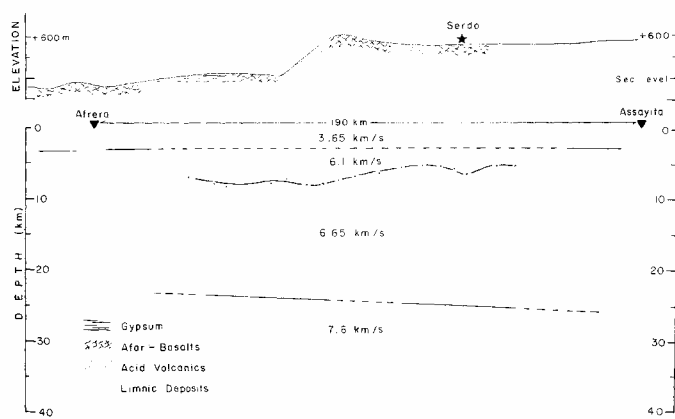


Fig. 108. Seismic depth-velocity meridional profile from Lake Afrera in the Depression to Assayita via Serdo obtained by Berckhemer et al. (1975) from deep soundings conducted in 1972 (adapted from Berckhemer 1975, Fig. 3 and 4, p. 99 and 101).

Layers	Depth (km)	Seismic velocity (km/s)
1	0-3	4.5
2	3-12	6.3
3	12-23	6.8
4	23-possibly 50*	7.4

\*The extension in depth of the low-velocity layer is deduced from the adjustment of observed-to-computed gravity data (Makris et al. 1975, p. 138).

**Fault Plane Solutions**— McKenzie et al. (1970) computed fault plane solutions for the two largest Serdo earthquakes, those of 29 March at U.T. 11:04.8 and 5 April at U.T. 18:30.7. The two epicentres were about 20 km apart and their solutions identical, namely a first nodal plane heading N63E with a 70° dip to the SE and a second plane striking N27W with a 90° dip (McKenzie et al. 1970, p. 243-248) (see Table 5, Fig. 109).

McKenzie et al. chose the NNW-SSE (333°) direction as the primary nodal plane because the left lateral strike-slip motion it indicated was consistent with the field reports by Gouin and Dakin (1969) on the direction of the fresh faults that the earthquakes had triggered and with the general trend of local surface faulting. Gouin (1975) adopted the same interpretation.

Fairhead and Girdler (1971), Girdler (1977, personal communication) selected the alternate 063° direction for the primary nodal plane. They based their argument on: (1) the eastnortheasterly alignment of the larger

Table 5. Fault plane solutions available in 1971 for northeast African epicentres.

Coordinates	m <sub>n</sub>	Plane striking ENE		Plane striking NNW	
		Strike	Dip	Strike	Dip
1967/III/13 N 19.79° E 38.72°	5.8	053°	82° SE	141°	83° NE
1962/XI/11 N 17.22° E 40.58°	5.6	049°	78° SE	141°	81° SW
1969/III/29 N 12.02° E 41.18°	5.8	063°	70° SE	153°	90°
1969/IV/05 N 12.19° E 41.13°	6.2	063°	70° SE	153°	90°
1959/XII/21 N 13.98° E 41.18°	6.7	030°	70° SE	123°	75° NE

#### Sources:

1967 and 1962 — Fairhead 1968; 1969 — McKenzie et al. 1970; and 1959 — Sykes (personal communication).

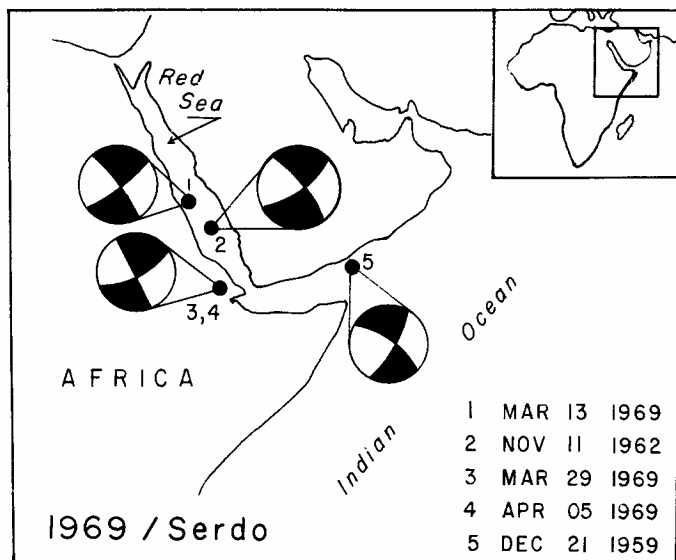


Fig. 109. Fault-plane solutions for five epicentres in the magnitude range  $5.6 < m_b < 6.7$  available for the region of northeastern Africa. The plots are equal area projections of the lower hemisphere of the focal sphere.

Serdo earthquakes, which is very apparent on the USCGS and JED epicentre distribution pattern (Fig. 104), but not so evident on the ISC distribution pattern; and (2) the postulated existence of an ENE-trending transform fault under the Bidu-Dubbi volcanic line that would have caused the separation of the Danakil horst from the Nubian tectonic plate and allowed the observed  $15^\circ$  counterclockwise rotation of the Danakil horst with respect to the rest of Africa. They argued that a SW-NE right lateral motion at depth, as revealed by the larger Serdo shocks, could have produced northwesterly left-lateral faults on the surface similar to those observed 8 km east of Serdo. Such an explanation certainly agrees with Anderson's rhombic fault pattern theory and is backed by laboratory experiments (Courtilot et al. 1974). However, the general surface faulting pattern in the Serdo region north of  $N 11.9^\circ$  and west of  $E 41.5^\circ$  does not suggest any such northeasterly trend. Anywhere else to the north or east of the 1969 seismic region boxed by dotted lines on Fig. 100, the assumption of such a northeasterly fault at depth, that is below the thin crust of Afar, would be strengthened by the presence of curvilinear and ENE trending geologic

structures. Even an idealized two-block laboratory model such as the one used by Courtilot et al., when progressively dislocated, leaves, on the surface of the clay layer that covers it, fault marks subparallel to the directions of the three sectors of the transform fault model (see Courtilot et al. 1974). Only the accurate plotting of aftershocks of a sequence in the same region by a local seismic network could reveal the identity of these fault planes. The same reasoning applies for the five almost identical solutions illustrated in Fig. 109.

*Frequency-Magnitude Distribution and Strain Release* — Fairhead and Girdler (1970) computed the frequency-magnitude ( $m_b$ ) relation for the 12 epicentres determined from teleseismic data; Dakin and Gouin (1975) computed the same relation for 251 events whose original  $M_L$  (AAE) magnitudes were converted to  $m_b$  by the empirical equation:  $M_L$  (AAE) =  $0.24 + 1.05 m_b$  (CGS). The results were practically the same:  $\log N = 4.71 - 0.76 m_b$  (Fairhead and Girdler);  $\log N = 4.62 - 0.73 m_b$  (Dakin and Gouin) (Fig. 110).

The mean value of the b-coefficient (about 0.75) found for the 1969 Serdo sequence corresponds to values obtained over continental rift zones (Karnik 1969; Hattori 1974) and over Eastern Africa in particular, even if the authors used different limits for the East African regions considered, different periods of sampling, and different magnitude ranges. The published values for this region are:

b	Sampling period (years)	Regions	Authors
0.65		Western Rift	Wohlenberg 1968
0.79		East African Rift	Wohlenberg 1968
0.77		East Africa	Kaila and Narain 1971
0.84	60	Ethiopia and Horn of Africa	Gouin 1975
0.62	100	Ethiopia and Horn of Africa	Gouin 1975
0.71	343	Ethiopia and Horn of Africa	Gouin 1975

*Other Source Parameters* — The seismic moment, source dimensions average dislocation, and stress drop were determined by Maasha and Molnar (1972) for the Serdo earthquake of 5 April 1969 using the theory devel-

oped by Brune (1970). A shear modulus  $\mu = 3.3 \times 10$  cgs units and a density  $\rho = 2.71 \text{ g cm}^{-3}$  were assumed. Maasha and Molnar's results were:

Moment:	P = $1.9(6) \times 10^{25} \text{ dynes cm}^{-1}$	} Average = 1.43
	S = $1.1(8) \times 10^{25} \text{ dynes cm}^{-1}$	
Corner frequency:	P = $1.95 \times 10^{-1} \text{ hz}$	
	S = $1.1(8) \times 10^{-1} \text{ hz}$	
Radii:	P = 11.0 km	} Average = 11.9
	S = 12.2 km	
Area:	450 km <sup>2</sup>	
Dislocation:	10 cm	
Stress drop:	3.4 bars	

The limits of confidence for these values are discussed by Maasha and Molnar (1972, p. 5737-39). Their conclusions on the low amplitude of the stress drops they observed during the Serdo earthquakes and others in the African rift system are worth noting. Low stress drop is characteristic of earthquakes caused by tectonic rifting along plate boundaries; higher stress drops accompany earthquakes that occur within tectonic plates where the crust is thicker and the strength of the material greater. From the gradual increase in stress drop from the Red Sea to South Africa, Maasha and Molnar concluded that the "northern part of the rift system marks a narrow zone of weakness separating two stable, aseismic plates, whereas the southern part of the rift is not such a plate boundary yet or a zone weakness . . ." (p. 5739).

### 1969/IX/26

On 26 September at U.T. 04:54.5, an earthquake of magnitude  $m_b$  5.1 occurred at the south end of the central trough of the Red Sea, northeast of the Dahlak Islands. Four teleseismic solutions are available; they agree within  $\pm 0.1^\circ$  in longitude and latitude. The adopted epicentre is the average value of the four solutions: N 16:46°, E 41.05°; it is plotted on Fig. 92.

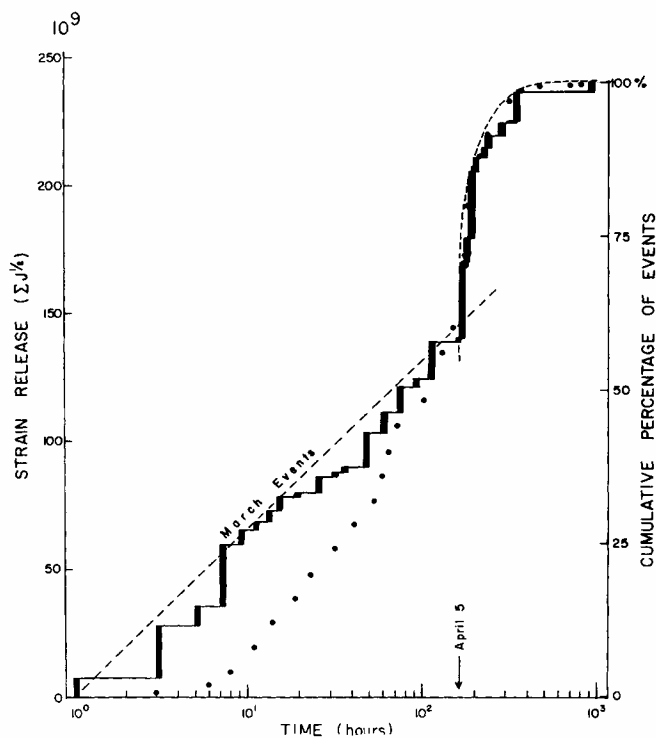


Fig. 110. Strain released during the 1969 March-April period of seismic activity (after Gouin 1971, p. 34).

#### Sources

BCIS; ISC (1969, p. 355-356); USCGS (EDR 63-69, p. 50).

#### Comments

As an evaluation of the earth models used by different agencies, it is to be noted that AAE recorded an  $iP(z)$  at 04:56:28.2 giving a P-H residual of only  $-0.6$  s for the CGS model as compared to  $-1.5$  s for the ISC model.